Journal of
Materials in Life Sciences

Vol. 5 No. 1 (2026)

Full Paper

Thiourea Ligand Coordination in Nickel(ii) and Zinc(ii) Complexes: Experimental and Computational Investigations

Nurul Fashila Binti Yanri[a], Fazira Ilyana Abdul Razak[a,b*], Roichatul Madinah[a], Yee Shi Wee[a]

[a]Department of Chemistry, Faculty of Science, Universiti Teknologi Malaysia, 81310 UTM Johor Bahru, Johor, Malaysia.
[b]Department of Physics, Faculty of Science and Technology, Universitas Airlangga, 60115 Surabaya, Indonesia

Article history
Received
28 February 2026
Revised
30 April 2026
Accepted
2 May 2026
Published online
30 May 2026

*Corresponding author
fazirailyana@utm.my

Abstract

Thiourea-based ligands exhibit versatile coordination behavior with transition metals; however, synthetic inconsistencies and unresolved structure–property profiles remain significant challenges in coordination chemistry. In this work, phenylthiourea (PTU) and N-(1-naphthyl)-N′-phenylthiourea (NPTU) were synthesized and coordinated with open-shell Ni(II) (d8) and closed-shell Zn(II) (d10) ions. The resulting complexes were characterized using ATR-FTIR, UV–Vis, and H NMR spectroscopy, complemented by density-functional theory and time-dependent DFT (TD-DFT) calculations to optimize molecular geometries and evaluate electronic features using B3LYP with 6-31G(d,p) and LANL2DZ. Spectroscopic and computational data confirmed successful coordination primarily through the thiocarbonyl sulfur atom. The Ni(II) complexes displayed pronounced red/blue structural shifts indicating strong covalent bonding, whereas Zn(II) complexes demonstrated weaker, mostly electrostatic interactions driven by its stable d10 configuration. Computational optimization aligned well with experimental results, confirming a square planar shape for Ni(II) and a tetrahedral geometry for Zn(II) complexes. This integrated approach successfully maps the coordination pathways of asymmetric thioureas, offering a reliable blueprint for predicting electronic properties in future material and life science applications.

Keywords : Coordination chemistry, Density-functional theory, Nickel(II) complexes, Thiourea, Zinc(II) complexes

© 2026 Penerbit UTM Press. All rights reserved

1.0 INTRODUCTION

The study of coordination compounds produced by the interaction of metal ions and ligands is a foundational pillar of inorganic chemistry [1-4]. A central metal ion typically binds to surrounding molecules or ligand ions via coordinate covalent bonds to form a coordination complex [5-6]. The physical and chemical characteristics of these complexes are directly influenced by the type of metal center [7], the specific donor atoms in the ligand [8], and the resulting coordination geometry [9]. In this study, nickel(II) and zinc(II) were selected to provide a comparative analysis between an open-shell d^8 and a closed-shell d^{10} system. This choice allows comparison between an open-shell d^8 Ni(II) system and a closed-shell d^{10} Zn(II) system, particularly in terms of metal–ligand electronic interactions and charge delocalization behavior.

Among the diverse range of investigated ligands, thiourea and its derivatives have garnered significant attention due to their strong donor capacity [10], coordination adaptability [11], and ease of structural modification [12]. According to Pearson's Hard and Soft Acids and Bases (HSAB) principle, thiourea can form stable complexes with both hard and soft metal

ions because its skeleton contains both sulfur (a soft donor atom) and nitrogen (a hard donor atom) [13]. For this project, phenylthiourea (PTU) and N-(1-naphthyl)-N′-phenylthiourea (NPTU) were chosen as ligands due to their extended aromatic systems and dual donor sites (S and N), which actively promote coordination with transition metals. These ligands can function as bidentate chelating agents through both thione (S-donor) and N-donor coordination, creating stable chelate rings that influence electron density distribution. Interestingly, these same ligands can also act as monodentate agents by coordinating through either the sulfur or nitrogen atom alone. The exact mode of coordination depends heavily on the specific metal ion chosen for complexation.

Although thiourea-derived metal complexes have been extensively reported, several key research gaps remain. First, the synthesis of thiourea-based nickel(II) and zinc(II) complexes—especially those utilizing asymmetrically substituted thiourea ligands—often suffers from low or inconsistent yields, high sensitivity to reaction conditions, and reproducibility issues [12,14-16]. Previous studies have demonstrated that changes in solvent polarity, metal salt precursors, reaction temperature, and ligand-to-metal ratios greatly impact complex formation and stability [17-18]. However, these synthetic constraints are frequently overlooked in current literature, making meaningful comparisons difficult because many reported thiourea compounds lack standardized, reliable preparation procedures. Given their versatility, optimizing the synthesis of these thiourea-based metal complexes is essential, as they serve as a solid foundation for future applications in chemical and material sciences.

Therefore, this work aims to investigate the coordination behavior of Zn(II) and Ni(II) ions toward thiourea-based ligands through the correlation of experimental characterization data and computational results. PTU and NPTU were synthesized and coordinated with Zn(II) and Ni(II) ions to form their corresponding metal complexes. Experimental characterization was performed using Fourier Transform Infrared (FTIR) spectroscopy, proton nuclear magnetic resonance (^{1}H NMR) spectroscopy, and UV–visible spectroscopy to evaluate ligand formation, coordination behavior, and changes in electronic transitions upon complexation. In addition, density-functional theory (DFT) and time-dependent DFT (TD-DFT) calculations were carried out to optimize molecular geometries and investigate the vibrational and electronic properties of the compounds. The combined experimental and computational approach was employed to provide further insight into the coordination characteristics and electronic behavior of the resulting metal complexes.

2.0 EXPERIMENTAL

2.1 Materials

All chemicals and reagents were used as received from commercial suppliers. 1-naphthyl isothiocyanate (95%), triethylamine (99.5%), ammonium thiocyanate (97.5%), aniline (99%), ethanol (95%), hydrochloric acid (1M, 97%), and ethyl acetate (99.8%) were purchased from Sigma-Aldrich. Nickel(II) acetate tetrahydrate [Ni(OAc)2.4H_2O] (98%) was supplied by QReC. Zinc chloride ($ZnCl_2$, 98%), n-hexane (98.5%), and dichloromethane (99.8%) were obtained from Supelco.

2.2 Synthesis of ligand and its metal complex

Synthesis of Anilinium Chloride

The synthesis of anilinium chloride began with the distillation of crude aniline (40 mL, 0.44 mol) in a 250 mL round-bottom flask. The crude aniline was mixed with distilled water (240 mL) and a 10% NaOH solution (15 mL, 1.5 g). The aniline distillate was collected in a receiver kept in an ice bath (0–5 °C) until the distillation was complete. The collected distillate was transferred into a separatory funnel and allowed to stand for 5 minutes. The aniline layer was then separated and dried over anhydrous potassium carbonate (2 g, 0.014 mol). A portion of this distilled aniline (20 mL, 0.22 mol) was transferred to a beaker and diluted with ethanol (60 mL). The mixture was stirred in an ice bath (0–5 °C) for 5 minutes, followed by the dropwise addition of 37% HCl (45 mL). The mixture was stirred in the ice bath for an additional 15 minutes. After complete precipitation of anilinium chloride, the product was filtered using a Buchner funnel and air-dried for 30–60 minutes. Finally, the anilinium chloride was transferred into a vial and weighed.

Synthesis phenylthiourea (PTU)

The ligand phenylthiourea (PTU) was synthesized by dissolving ammonium thiocyanate (0.76 g, 0.01 mol) in 15 mL of distilled water in a round-bottom flask. Anilinium chloride (1.5 g, 0.01 mol) was subsequently added to the solution, and the resulting mixture was heated under reflux at 180°C for 1.5 h. The progress of the reaction was monitored by thin-layer chromatography (TLC) using a 1:1 (v/v) mixture of ethyl acetate and n-hexane as the mobile phase. Upon completion, the mixture was cooled to room temperature and then kept in an ice bath for 15 min to induce precipitation. The resulting precipitate was collected via filtration using a Büchner funnel, air-dried, and further dried in a desiccator to yield the pure ligand.

Synthesis of Diacetatobis(phenylthiourea) nickel(II) (Ni-PTU)

The nickel complex was prepared by dissolving the PTU ligand (1.0 mmol) in 20 mL of hot ethanol. Separately, $Ni(OAc)_2 . 4H_2O$ (0.5 mmol) was dissolved in 15 mL of ethanol. The metal salt solution was added dropwise to the ligand solution under continuous stirring at 60°C. The reaction mixture was stirred for an additional 2 h and then allowed to cool to room temperature. The resulting precipitate was filtered, washed sequentially with chilled ethanol and diethyl ether, and finally dried at 40°C.

Synthesis of N-(1-naphthyl)-N'-phenylthiourea (NPTU)

The ligand N-(1-naphthyl)-N'-phenylthiourea (NPTU) was synthesized by dissolving 1-naphthyl isothiocyanate (0.185 g, 1.0 mmol) in 10 mL of dichloromethane (DCM) in a 50 mL round-bottom flask, which was then cooled in an ice bath to 0°C. In a separate vessel, aniline (0.10 mL, 1.1 mmol) and triethylamine (0.17 mL) were dissolved in 2 mL of DCM. This solution was added dropwise to the chilled isothiocyanate solution at 0°C. The reaction mixture was stirred at 0°C for 30–60 min, allowed to warm to room temperature, and stirred for another 30–60 min. Reaction completion and product formation were confirmed via TLC analysis.

S***ynthesis of Dichloridobis-(N-(1-naphtyl)-N'-phenylthiourea) Zinc(II) (Zn-NPTU)***

The zinc complex was synthesized via a one-pot method continuing directly from the freshly prepared NPTU ligand solution. Following TLC confirmation of ligand formation, 15 mL of ethanol was added to the reaction mixture. Separately, $ZnCl_2$ (0.124 g, 0.50 mmol) was dissolved in 5 mL of ethanol and introduced into the reaction flask. The mixture was stirred and heated within a temperature range of 40°C to 50°C for 2 h, during which a green solution was observed. The mixture was allowed to stand at room temperature to precipitate the complex. The product was then isolated by filtration using a Büchner funnel, washed with 10 mL of ethanol followed by distilled water, and dried.

2.4 Characterization

Proton Nuclear Magnetic Resonance Spectroscopy (^{1}H NMR)

NMR spectroscopy was employed to elucidate the molecular structure by analyzing the number and chemical environments of proton atoms within the compounds. The spectra were recorded using a Bruker Model Avance II 400 MHz NMR spectrophotometer operating at a radiofrequency of 400 MHz. Deuterated chloroform ($CDCl_3$) was used as the solvent for the ligand and Zn(II) complex, whereas dimethyl sulfoxide (DMSO-d_6) was used for the Ni(II) complex. The chemical shifts (δ) were recorded in parts per million (ppm) and used for structural characterization of the synthesized compounds.

Fourier Transform Infrared Spectroscopy (FTIR)

Attenuated Total Reflectance–Fourier Transform Infrared (ATR-FTIR) spectroscopy was employed to identify the organic functional groups present in the ligand and metal complexes. The FTIR spectra was recorded using a PerkinElmer Series 1600 FTIR spectrometer equipped with an ATR accessory. In this technique, the infrared beam was directed onto the ATR crystal at an angle greater than the critical angle, resulting in multiple internal reflections at the crystal interface. The absorption spectra of the compounds were recorded over the range of 4000–400 cm^{-1} for functional group characterization.

Ultraviolet–Visible Spectroscopy (UV–Vis)

Ultraviolet–visible (UV–Vis) spectroscopy was performed to analyze the electronic absorption characteristics of the ligand and metal complexes. The spectra were recorded using a Shimadzu Corporation UV-1800 spectrophotometer. The ligand solution was prepared in dichloromethane (DCM) at a concentration of 1×10^{-12} M, whereas the metal complexes were prepared in chloroform at a concentration of 1×10^{-9} M. The electronic absorption spectra of the compounds were recorded over the wavelength range of 200–800 nm.

2.3 Computational method

The geometrical and electronic properties of the zinc(II) and nickel(II) complexes were investigated using density-functional theory (DFT) calculations performed with the Gaussian 16 software package [19]. The B3LYP functional was employed due to its reliability in describing transition-metal systems [20–23]. The 6-31G basis set was used for H, C, N, and S atoms, whereas the LANL2DZ basis set together with the corresponding effective core potential (ECP) was employed for the Ni(II) and Zn(II) atoms. The use of a mixed basis set is a common practice for transition-metal complexes, where the 6-31G basis set is employed for the ligand atoms and LANL2DZ is used for the Ni(II) and Zn(II) atoms. The molecular structures were fully optimized in the gas phase to obtain the minimum-energy geometries, from which structural parameters were obtained. Gas-phase calculations were adopted to obtain optimized geometries and electronic structures for qualitative interpretation of the experimental spectroscopic data and consistent comparison of the investigated compounds.

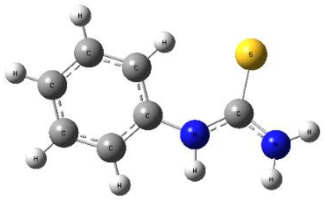
Time-dependent density-functional theory (TD-DFT) calculations were subsequently performed at the same level of theory as the geometry optimization to investigate the electronic transitions of the metal complexes. Seven excited states were calculated to simulate the UV–Vis absorption spectra, analyze the frontier molecular orbitals (FMO), and investigate the nature of the electronic transitions. Vibrational frequency calculations were carried out on the optimized geometries using the same level of theory. The calculated FTIR spectra was used to evaluate the vibrational properties of the synthesized compounds and to examine changes in vibrational frequencies following complex formation.

3.0 RESULTS AND DISCUSSION

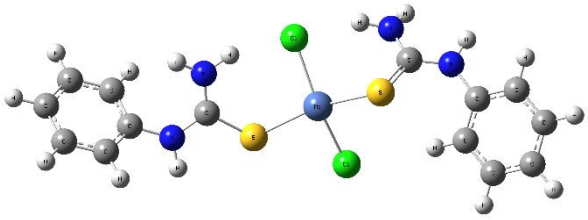
Phenylthiourea (PTU) and N-(1-naphthyl)-N′-phenylthiourea (NPTU) were successfully synthesized as white and whitish-brown powders with yields of 2.43% and 99.0%, respectively (see Figure S1 in Supporting Information). Meanwhile, the corresponding metal complexes, Diacetatobis(phenylthiourea)nickel(II) (Ni-PTU) and Dichlorodobis(N-(1-naphthyl)-N′-phenylthiourea)zinc(II) (Zn-NPTU), were obtained as green and white solids with yields of 89.01% and 22.35%, respectively (see Figure S2).

3.1 The optimized structure of ligands and its metal complex

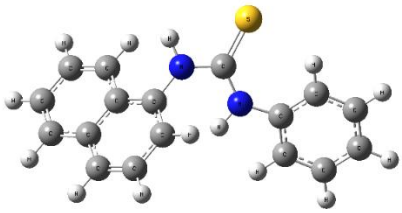
Figure 1 presents the optimized geometries of the studied ligands and their corresponding metal complexes (PTU and Ni–PTU; NPTU and Zn–NPTU), together with their calculated dipole moments. Geometry optimizations were performed for the possible spin states of each system, and the lowest-energy configuration was selected for subsequent analyses. As summarized in Table S1 (Supporting Information), all optimized ground-state structures correspond to the singlet spin state. The optimized geometries are also consistent with the coordination geometries reported for structurally related thiourea metal complexes, in which Ni(II) preferentially adopts a square-planar geometry [24], whereas Zn(II) typically forms tetrahedral complexes [25,26]. Moreover, in general, the dipole moments increased slightly upon complex formation, indicating changes in molecular polarity and electron distribution following coordination with the metal ions. Among the optimized structures, the $Zn(NPTU)_2$ complex exhibited the highest dipole moment (8.185 D), suggesting a comparatively greater degree of charge separation and molecular asymmetry relative to the free ligands and the other optimized complexes.



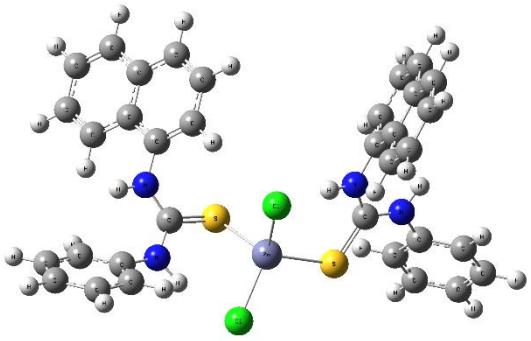
(a) PTU, 5.49 D



(b) Ni-PTU, 5.63 D



(c) NPTU, 5.97 D



(d) Zn-NPTU, 8.18 D

Figure 1 : The optimized structure of ligand and its metal complexes: (a) PTU, (b) Ni-PTU, (c), NPTU, and (d) Zn-NPTU, as well as their dipole moment values

3.2 Infrared Spectroscopy: ATR-FTIR Spectrum and TD-DFT results

The calculated FTIR spectra showed reasonable agreement with the experimental vibrational frequencies, as summarized in Table 1. This agreement indicates that the DFT calculations adequately reproduced the major vibrational features of the synthesized compounds. The experimental C=S stretching vibrations of PTU and NPTU were observed at 1229.00 and 1241.40

cm^{-1}, respectively, while the corresponding calculated frequencies were 1134.62 and 1231.13 cm^{-1}. Upon coordination, the C=S stretching frequencies shifted to 1261.56 cm^{-1} for Ni–PTU and 1195.05 cm^{-1} for Zn–NPTU, with calculated values of 1242.62 and 1198.69 cm^{-1}, respectively. The deviations between the experimental and calculated frequencies were generally below 10%, demonstrating reasonable agreement between theory and experiment.

Table 1 : Experimental and computational results of ATR-FTIR for ligand and complexes (in cm^{-1}). The detailed FTIR spectra can be seen in Figure S3

No.	Compound	Mode	N–H	C=S	C=C
1.	PTU	Experimental	3419.90	1229.00	1607.57
		Computational	3563.15	1134.62	1667.25
		%Deviation	4.02	8.31	3.58
2.	NPTU	Experimental	3201.36	1241.40	1597.67
		Computational	3242.84	1631.13	1198.67
		%Deviation	1.28	2.38	3.32
3.	Ni-PTU	Experimental	3420.58	1261.56	1607.63
		Computational	3234.21	1242.62	1647.23
		%Deviation	5.76	1.52	2.59
4.	Zn-NPTU	Experimental	3145.06	1195.05	1645.94
		Computational	3312.45	1198.69	1634.00
		%Deviation	5.05	0.30	0.73

The vibrational analysis revealed different coordination behavior for the Ni(II) and Zn(II) complexes, particularly through changes in the C=S stretching frequencies [27,28] The N–H stretching frequencies of PTU and NPTU also differed slightly, which may be attributed to differences in hydrogen-bonding interactions and the greater π-conjugation introduced by the naphthyl substituent in NPTU. For the PTU ligand and its Ni(II) complex, the C=S stretching vibration shifted from 1229.00 cm^{-1} to 1261.56 cm^{-1} after coordination, corresponding to a blue shift. This shift may be associated with disruption of intermolecular hydrogen-bonding interactions in the free ligand together with redistribution of electron density upon coordination to the Ni(II) center, resulting in an increase in the C=S stretching frequency. In contrast, the NPTU ligand and its Zn(II) complex exhibited a red shift in the C=S stretching vibration, where the absorption band decreased from 1241.40 cm^{-1} to 1195.05 cm^{-1} upon complexation. This decrease is consistent with sulfur coordination to the Zn(II) center, which may reduce the double-bond character of the C=S bond through electron density donation from sulfur to the metal ion. A corresponding red shift was also observed for the N–H stretching vibration, indicating changes in the local electronic and hydrogen-bonding environment after coordination. Overall, the observed vibrational shifts, together with the reasonable agreement between the experimental and calculated spectra, support the proposed coordination of the thiourea ligands to the metal ions [27].

3.3 ^{1}H NMR Spectroscopy analysis

The major signals observed in the ^{1}H NMR spectra correspond to the NH protons of the thiourea moiety and the aromatic protons of the phenyl and naphthyl rings (Figure S4). The chemical shifts are summarized in Table 2. The ^{1}H NMR spectrum of PTU, recorded in $CDCl_3$, displayed NH proton signals at δ 7.904 ppm (NH_a) and δ 7.884 ppm (NH_b), while the aromatic protons appeared as multiplets in the range of δ 7.431–7.356 ppm. Similarly, the spectrum of NPTU showed NH proton signals at δ 7.531 ppm (NH_a) and δ 7.512 ppm (NH_b), with aromatic proton resonances observed between δ 7.413–7.335 ppm. The downfield positions of the NH signals are attributed to the deshielding effect of the adjacent nitrogen atom within the thiourea moiety.

Upon complexation, further downfield shifts of the NH proton signals were observed, indicating a reduction in electron density around the NH protons following coordination to the metal centers. Although coordination is proposed to occur primarily through the sulfur atom, the observed NH chemical shifts suggest that metal coordination influences the electronic environment of the entire thiourea moiety, consistent with previous studies on thiourea-based metal complexes [29]. In Ni–PTU, the NH proton signal shifted to δ 9.802 ppm, while the aromatic proton resonances appeared in the range of δ 7.405–7.284 ppm. Similarly, in Zn–NPTU, the NH proton resonance shifted downfield to δ 8.028 ppm, and the aromatic proton signals were

observed between δ 7.587–7.475 ppm. These spectral changes are consistent with coordination of the ligands to the respective metal ions and with the redistribution of electron density upon complex formation.

Table 2 : Experimental data of NMR for ligand and complexes in δ (ppm)

No.	Compound	$NH_{(a)}$	$NH_{(b)}$	H−Ar
1.	PTU	7.904	7.884	7.431−7.356
2.	NPTU	7.531	7.512	7.413−7.335
3.	Ni-PTU	9.802	-	7.405−7.284
4.	Zn-NPTU	8.028	8.008	7.587−7.475

3.4 UV–Visible Spectroscopy and TD-DFT Results

The UV–Vis absorption spectra of the synthesized ligands and their corresponding metal complexes were recorded in the wavelength range of 230–400 nm to evaluate their electronic transition behavior and metal–ligand interactions. The experimental and theoretical absorption data, including the maximum absorption wavelengths and oscillator strengths, are summarized in Table 3 (The detailed UV–Vis absorption spectra can be seen in Figure S5). Theoretical calculations were performed using TD-DFT to support the interpretation of the experimental spectra. For PTU, an absorption band was observed at 269 nm and assigned to a ligand-centered π→π* transition. This assignment is consistent with previous studies on thiourea derivatives and related transition-metal complexes, where the high-energy absorption bands are attributed to π→π* excitation within the conjugated ligand framework [29-31]. Upon coordination with Ni(II), the absorption maximum of Ni–PTU shifted slightly to 267.5 nm, indicating that metal coordination modifies the electronic environment of the ligand. Similarly, NPTU exhibited an absorption band at 272.5 nm, which was also assigned to a ligand-centered π→π* transition. Compared with PTU, the slightly longer absorption wavelength of NPTU is consistent with the larger π-conjugated naphthyl system, which lowers the energy required for the π→π* transition. Similar observations have been reported for aromatic thiourea derivatives containing extended conjugated systems [31].

Table 3 : Experimental and computational data of UV-Vis for ligand and complexes

No.	Compound	Mode	λ_{max} (nm)	Abs/Oscillator Strength
1.	PTU	Experimental	269.00	1.325
		Computational	232.92	0.1354
2.	NPTU	Experimental	272.50	1.788
		Computational	324.99	0.1841
3.	Ni-PTU	Experimental	267.50	1.123
		Computational	349.48	0.1062
4.	Zn-NPTU	Experimental	263.50	1.246
		Computational	307.02	0.246

Additional absorption bands observed after complexation are consistent with charge-transfer transitions commonly reported for related thiourea metal complexes, providing further evidence of metal–ligand coordination [29]. The oscillator strength (f), which reflects the probability of electronic transitions, was generally higher for the free ligands than for the corresponding metal complexes. This observation suggests that metal coordination influences the electron distribution within the thiourea framework, thereby affecting the probability of the electronic transitions. Although slight discrepancies were observed between the experimental and calculated absorption wavelengths, these differences are expected because the calculations were performed in the gas phase, whereas the experimental spectra were recorded in solution. Solvent effects and thermal broadening may therefore contribute to the observed differences. Nevertheless, the overall agreement between the experimental UV–Vis spectra and the TD-DFT calculations supports the proposed electronic structures of the synthesized compounds and provides complementary evidence for metal–ligand coordination.

3.5 Correlation of experimental and computational studies

The experimental spectroscopic results and the DFT calculations consistently support the proposed coordination structures of the synthesized metal complexes. The FTIR spectra showed coordination-induced shifts in the v(C=S) and v(C–N) vibrational bands, while the ^{1}H NMR spectra exhibited downfield shifts of the NH proton signals following complexation. These observations are in good agreement with the DFT-optimized geometries, which showed elongation of the C=S bond upon coordination together with the formation of metal–sulfur bonds. In contrast, the relatively long M···N distances obtained from the optimized structures suggest that sulfur is the primary coordination site in both complexes. Furthermore, the TD-DFT calculations reproduced the overall trend of the experimental UV–Vis spectra, providing additional support for the proposed electronic structures despite the small differences in the calculated and experimental absorption wavelengths.

Comparison of the two metal complexes revealed distinct coordination behavior that is consistently reflected in both the experimental and computational results. The Ni–PTU complex exhibited larger shifts in the FTIR and ^{1}H NMR spectra than the Zn–NPTU complex, indicating a greater perturbation of the ligand electronic environment following coordination. This observation is consistent with the shorter calculated Ni–S bond length (2.328 Å) compared with the Zn–S bond length (2.441 Å), see Table S2, suggesting stronger metal–sulfur interactions in the Ni(II) complex. In contrast, the comparatively smaller spectroscopic changes observed for the Zn(II) complex are consistent with the longer Zn–S bond length obtained from the optimized geometry.

Overall, the combined experimental and computational results consistently support coordination through the thiocarbonyl sulfur atom for both complexes. The integrated spectroscopic and DFT analyses indicate that the proposed square-planar geometry for the Ni–PTU complex and tetrahedral geometry for the Zn–NPTU complex provide the best description of the synthesized compounds. The reasonable agreement between the experimental observations and the computational results demonstrates that the DFT and TD-DFT calculations employed in this study provide a reliable qualitative description of the structural and electronic properties of these thiourea-based metal complexes.

4.0 CONCLUSION

The synthesis of thiourea-based ligands, namely phenylthiourea (PTU) and N-(1-naphthyl)-N′-phenylthiourea (NPTU), together with their corresponding Zn(II) and Ni(II) complexes, was successfully carried out. The formation of the metal complexes was supported by observable physical changes, including differences in color and product yield, particularly for Diacetatobis(phenylthiourea)nickel(II), Ni-PTU, which was obtained as a green powder with a yield of 89.01%. Spectroscopic characterization using FTIR, ^{1}H NMR, and UV–Vis spectroscopy provided evidence for metal–ligand coordination. The FTIR spectra showed shifts in the v(C=S) stretching vibrations after complex formation, suggesting the involvement of the thiourea sulfur atom in coordination. Changes in the ^{1}H NMR chemical shifts of the NH protons further indicated alterations in the electronic environment upon coordination, while the UV–Vis spectra demonstrated changes in the electronic absorption behavior of the ligands after interaction with the metal ions.The DFT and TD-DFT calculations were generally consistent with experimental observations. Geometry optimization provided stable molecular structures and theoretical vibrational frequencies that followed trends similar to those observed experimentally. The calculated geometries also supported the formation of metal–ligand interactions involving the thiourea donor atoms. Overall, the combined experimental and computational results suggest that both Ni(II) and Zn(II) complexes coordinate predominantly through the sulfur atom of the thiourea ligands. The spectroscopic and computational data further indicate that the Ni(II) complex exhibits relatively stronger metal–ligand interaction compared to the Zn(II) complex, which may be associated with differences in their electronic configurations.

Acknowledgment

This project was funded by the Ministry of Higher Education, Malaysia, for the Fundamental Research Grant Scheme FRGS (PY/2025/02278/R.J130000.7854.5F764). Author thanks the Centre for Information and Communication Technology (CICT), Universiti Teknologi Malaysia for supporting and providing high-performance computing facilities and services that expedited the research.

References

[1] Turel, I. (2015). Special issue: Practical applications of metal complexes. *Molecules*, 20(5), 7951–7956. https://doi.org/10.3390/molecules20057951

[2] Mohammed, H. S., & Tripathi, V. D. (2020). Medicinal applications of coordination complexes. *Journal of Physics: Conference Series*, 1664(1), 012070. https://doi.org/10.1088/1742-6596/1664/1/012070

[3] Tong, M. L., & Chen, X. M. (2017). Synthesis of coordination compounds and coordination polymers. In *Modern inorganic synthetic chemistry* (2nd ed., pp. 189–217). Elsevier. https://doi.org/10.1016/B978-0-444-63591-4.00008-2

[4] Housecroft, C. E. (2018). *Chemistry: An introduction to organic, inorganic and physical chemistry* (4th ed.). Pearson.

[5] Aziz, K. N., Ahmed, K. M., Omer, R. A., Qader, A. F., & Abdulkareem, E. I. (2024). A review of coordination compounds: Structure, stability, and biological significance. *Reviews in Inorganic Chemistry*. https://doi.org/10.1515/revic-2024-0035

[6] Amouri, H., & Gruselle, M. (2009). *Chirality in transition metal chemistry: Molecules, supramolecular assemblies and materials*. Springer.

[7] Guo, L., Yang, Z., Dong, H., Lai, K., Fu, H., Gong, Y., Li, S., Yue, M., & Liu, Z. (2025). Systematic investigation of coordination chemistry in iridium(III) and ruthenium(II) complexes derived from pyridyl–amine ligands and their anticancer evaluation. *Inorganic Chemistry*, 64(21), 10379–10401. https://doi.org/10.1021/acs.inorgchem.4c05599

[8] Liu, Y., Pan, M., Li, K., Yan, C., Shen, Y., Zhao, C., Wang, W., & Su, C. (2011). Metal-directed assembly of hexameric ring, dimeric ring and 1D chain from a branched tripodal ligand. *Crystal Growth & Design*, 11(11), 4876–4884. https://doi.org/10.1021/cg200701j

[9] Schweinfurth, D., Demeshko, S., Sommer, M. G., Dechert, S., Meyer, F., & Sarkar, B. (2016). FeII and CoII complexes with click-derived tripodal ligands: Influence of the peripheral substituents on geometric structures and magnetic properties. *European Journal of Inorganic Chemistry*, 2016(15–16), 2581–2585. https://doi.org/10.1002/ejic.201501385

[10] Zborovskii, Y., Orysyk, V., Orysyk, S., & Vovk, M. (2025). Functionalized thioureas in medicinal chemistry: Binding ability of thiourea derivatives to biological targets, focused on their anticancer activity. *Biointerface Research in Applied Chemistry*, 15(2), 023. https://doi.org/10.33263/BRIAC152.023

[11] Lapasam, A., & Kollipara, M. R. (2020). A survey of crystal structures and biological activities of platinum group metal complexes containing N-acylthiourea ligands. *Phosphorus, Sulfur, and Silicon and the Related Elements*, 195(10), 789–812. https://doi.org/10.1080/10426507.2020.1764956

[12] Al-Riyahee A, Shanta A, Dhaef H. (2022). First Row Transition Metal Complexes Derived from N, N '-Substituted Thiourea: Synthesis, Geometrical Structures and Cyclic Voltammetry Probe: A Review. *Dalton Transactions*, 51(9), 3531–3545. https://doi.org/10.1039/D1DT04091J

[13] Pearson, R. G. (1963). Hard and soft acids and bases. *Journal of the American Chemical Society*, 85(22), 3533–3539.

[14] Risi, M. C. (2024). A review of the synthesis and coordination of some lesser studied thiourea ligands bearing electronegative sulfonyl, phosphoryl and cyano substituents towards platinum group and related metal centers. *Journal of Coordination Chemistry*, 77(1–2), 1–25. https://doi.org/10.1080/00958972.2024.2407665

[15] Ahmed, M. M., Salama, N. T. I., Bondock, S., Soayed, A. A., & Elsamra, R. M. I. (2025). Synthesis, spectroscopic characterization, DFT calculations, and molecular docking of novel thiourea complexes and their cytotoxic and antimicrobial activities. *Applied Organometallic Chemistry*, 39(4), e70125. https://doi.org/10.1002/aoc.70125

[16] Yeşilkaynak, T., Özkömeç, F., Çeşme, M., Demirdöğen, R., Kutlu, E., Kutlu, H., & Emen, F. (2022). Synthesis of new thiourea derivatives and metal complexes: Thermal behavior, biological evaluation, in silico ADMET profiling and molecular docking studies. *Journal of Molecular Structure*, 1269, 133758. https://doi.org/10.1016/j.molstruc.2022.133758

[17] De Marco, D., & Zona, G. (2007). Complex formation equilibria between Ag(I) and thioureas in n-propanol. *Thermochimica Acta*, 452(1), 82–84. https://doi.org/10.1016/j.tca.2006.06.017

[18] Joshaghani, M., Gholivand, M. B., & Ahmadi, F. (2008). Spectrophotometric and conductometric study of complexation of salophen and some transition metal ions in nonaqueous polar solvents. *Spectrochimica Acta Part A: Molecular and Biomolecular Spectroscopy*, 70(5), 1073–1078. https://doi.org/10.1016/j.saa.2007.10.015

[19] Frisch, M. J., Trucks, G. W., Schlegel, H. B., Scuseria, G. E., Robb, M. A., Cheeseman, J. R., Scalmani, G., Barone, V., Petersson, G. A., Nakatsuji, H., Li, X., Caricato, M., Marenich, A. V., Bloino, J., Janesko, B. G., Gomperts, R., Mennucci, B., Hratchian, H. P., Ortiz, J. V., Izmaylov, A. F., Sonnenberg, J. L., Williams-Young, D., Ding, F., Lipparini, F., Egidi, F., Goings, J., Peng, B., Petrone, A., Henderson, T., Ranasinghe, D., Zakrzewski, V. G., Gao, J., Rega, N., Zheng, G., Liang, W., Hada, M., Ehara, M., Toyota, K., Fukuda, R., Hasegawa, J., Ishida, M., Nakajima, T., Honda, Y., Kitao, O., Nakai, H., Vreven, T., Throssell, K., Montgomery, J. A., Jr., Peralta, J. E., Ogliaro, F., Bearpark, M. J., Heyd, J. J., Brothers, E. N., Kudin, K. N., Staroverov, V. N., Keith, T. A., Kobayashi, R., Normand, J., Raghavachari, K., Rendell, A. P., Burant, J. C., Iyengar, S. S., Tomasi, J., Cossi, M., Millam, J. M., Klene, M., Adamo, C., Cammi, R., Ochterski, J. W., Martin, R. L., Morokuma, K., Farkas, O., Foresman, J. B., & Fox, D. J. (2016). Gaussian 16 Revision C.01 [Computer software]. Gaussian, Inc.

[20] Zayed, E. M., El-Samahy, F. A., & Mohamed, G. G. (2019). Structural, spectroscopic, molecular docking, thermal and DFT studies on metal complexes of bidentate orthoquinone ligand. *Applied Organometallic Chemistry*, 33(9), e5065. https://doi.org/10.1002/aoc.5065

[21] Aly, A. A., Abdallah, E. M., Ahmed, S. A., Awad, M. K., Rabee, M. M., Mostafa, S. M., & Bräse, S. (2023). Metal complexes of new thiocarbohydrazones of Cu(I), Co(II), and Ni(II); identification by NMR, IR, mass, UV spectra, and DFT calculations. *Journal of Sulfur Chemistry*, 44(3), 282–303. https://doi.org/10.1080/17415993.2022.2145846

[22] Hashem, H. E., Mohamed, E. A., Farag, A. A., Negm, N. A., & Azmy, E. A. M. (2021). New heterocyclic Schiff base-metal complex: Synthesis, characterization, density functional theory study, and antimicrobial evaluation. *Applied Organometallic Chemistry*, 35(9), e6322. https://doi.org/10.1002/aoc.6322

[23] Muhmood, A. A., & AL-Temimei, F. A. (2019). New ruthenium metal complexes for their activity with DNA and cells of cancer/DFT-B3LYP calculations. *Indian Journal of Public Health Research & Development*, 10(6), 1240–1244. https://doi.org/10.5958/0976-5506.2019.01463.3

[24] Binzet G, Kavak G, Külcü N, Özbey S, Flörke U, Arslan H (2013) Synthesis and Characterization of Novel Thiourea Derivatives and Their Nickel and Copper Complexes. J Chem 2013:536562. https://doi.org/10.1155/2013/536562

[25] Srinivasan BR, Naik TA, Tylczyński Z, Priolkar KR (2014) Reinvestigation of growth of thiourea urea zinc sulfate crystal. Spectrochim Acta A Mol Biomol Spectrosc 118:1224–1228. https://doi.org/10.1016/j.saa.2013.08.083

[26] Kuchar J, Homzova K, Tomcik P, Culkova E, Vargova Z, Gyoryova K (2024) Synthesis, spectral, thermal properties, and crystal structure of bis(2,4-dichlorobenzoato-O)bis(thiourea-S)zinc(II). J Therm Anal Calorim 149(3):1125–1132. https://doi.org/10.1007/s10973-023-12653-9

[27] Limban C, Marutescu L, Chifiriuc MC (2011) Synthesis, Spectroscopic Properties and Antipathogenic Activity of New Thiourea Derivatives. Molecules 16(9):7593-7607. https://doi.org/10.3390/molecules16097593

[28] Al-Halbosy ATF, Hamada AA, Faihan AS, Saleh AM, Yousef TA, Abou-Krisha MM, Alhalafi MH, Al-Janabi ASM (2023) Thiourea Derivative Metal Complexes: Spectroscopic, Anti-Microbial Evaluation, ADMET, Toxicity, and Molecular Docking Studies. Inorganics 11(10):390. https://doi.org/10.3390/inorganics11100390

[29] Jasmani S, Jillani M, Sapari S, Razak FIA (2024) Synthesis and Characterization of Transition Complexes of Mono Thiourea as Ligand and Its Nonlinear Optic Application. J. Mater. Life Sci. 3(2) 67-77

[30] Tong KM, Toigo J, Patrick BO, Wolf MO (2023) Rhenium(I) Complexes with Sulfur-Bridged Dipyridyl Ligands: Structural, Photophysical, and Computational Studies. Inorg Chem 62(33):13662-13671. https://doi.org/10.1021/acs.inorgchem.3c02124

[31] Goh HY (2024) Synthesis, Structural Characterization, and Analysis of DFT and TD-DFT for IR and UV-Vis of Benzoyl Thiourea Ligand as Colorimetric Chemosensor. Final Year Project, Tunku Abdul Rahman University of Management and Technology. https://eprints.tarc.edu.my/29821/